

LASER GYROSCOPES

https://doi.org/10.1070/QEL17991

Output characteristic of four-frequency Zeeman laser gyroscope with an alternating frequency bias

Yu.Yu. Kolbas, Ya.S. Pyatnitskii, M.I. Rodionov, I.I. Saveliev

Abstract. **We have experimentally studied the output characteristic of a four-frequency Zeeman laser gyroscope (ZLG) on longitudinal modes with orthogonal circular polarisations having an alternating frequency bias and compared it with the output characteristic of a two-frequency ZLG. It is shown that by representing a four-frequency ZLG as a set of two-frequency ZLGs with orthogonal polarisations, the output characteristic of a four-frequency ZLG can be obtained through the arithmetic mean of the output characteristics of the same gyroscope. The experimental output characteristic of a four-frequency ZLG with an alternating bias in the form of a meander with a switching frequency of 1 kHz, as well as its combination with a low-frequency meander with a frequency of 1 Hz, is presented. The efficiency of using slow meander modulation for the linearization of the output characteristic of a four-frequency ZLG is demonstrated.**

Keywords: *laser gyroscope, Zeeman effect, four-frequency laser gyroscope, alternating frequency bias, output characteristic.*

1. Introduction

Zeeman laser gyroscopes (ZLGs) operating in the four-frequency (two-mode) generation regime potentially have a number of advantages compared to two-frequency (single-mode) ZLGs [1, 2]. These include a radical reduction in magnetic sensitivity, elimination of errors correlated in modes, a twofold decrease in the pulse value, and a reduction in quantum noise.

However, until now, the characteristics of four-frequency ZLGs (FZLGs) have been poorly studied experimentally, unlike two-frequency ZLGs, to which many works have been dedicated. Among the reasons are the complexity of the design of a four-frequency laser, the functional electronic circuit of its service life, and information processing algorithms. The literature only contains experimental estimates of the FZLG accuracy according to the Allan variation [3], estimates of the magnetic sensitivity [4], and the output characteristic in the absence of a frequency bias or with a constant frequency bias [5]. The four-frequency ZLG, in contrast to its Faraday analogue [6], is currently implemented only with an alternating-sign frequency bias [1, 3], since only in this case it is possible to design a high-precision perimeter stabilisation system providing acceptable gyroscope parameters [7]. For this reason, the output characteristic of a FZLG with an alternating frequency bias is of not only of scientific, but also of practical interest. The aim of this work is to experimentally study the output characteristic of an FZLG with an alternating frequency bias and compare it with the output characteristic of a two-frequency ZLG.

Yu.Yu. Kolbas, Ya.S. Pyatnitskii, M.I. Rodionov, I.I. Saveliev JSC M.F. Stelmakh Polyus Research Institute, ul. Vvedenskogo 3, korp. 1, 117342 Moscow, Russia; e-mail: i.saveliev@gmail.com

Received 10 September 2021; revision received 6 November 2021
Kvantovaya Elektronika **52** (2) 202–206 (2022)
Translated by M.A. Monastyrskiy

2. Description of the experiment

We have studied the output characteristic of a FZLG with an alternating-sign frequency bias described in [7]. The four-frequency ZLG operated in a four-pulse logic regime; the pulse value with regard to quadrupling was 0.75″. The half-widths of the static locking bands measured at the entrance to the lock were as follows: for the right-hand circular polarisation $\Omega^{r}_{L+} \approx 290$ Hz, for the left-hand one, $\Omega^{l}_{L+} \approx 310$ Hz. We used a rectangular alternating frequency bias in the form of a meander with an amplitude of $A = 5400$ Hz and a zero constant component. The frequency bias was switched with a period of $T = 1$ ms and a switching front of $\tau = 5$ μs at a level of 0.9. To desynchronise dynamic bands, amplitude modulation of the frequency bias in the form of a meander was used with a much smaller amplitude of $A_{sm} = 200$ Hz, and a much longer period of $T_{sm} = 1$ s. Further, for convenience, the meander of the fundamental frequency bias will be called the fast meander (FM), and the meander of the low-frequency amplitude modulation of the frequency bias will be called the slow meander (SM). The frequency bias was produced using a nonreciprocal device, which was formed by a solenoid wound on an active working channel; an alternating-sign current of the corresponding amplitude with the FM shape was passed through the solenoid [7]. A second solenoid was wound on top of this solenoid, through which an alternating-sign current was passed for low-frequency amplitude modulation of the frequency bias with the SM shape.

The polarising photomixer allowed isolation of the signal of each of the orthogonal modes, which, in turn, made it possible to visually compare the output characteristics of a four-frequency gyroscope and a single-mode gyroscope when representing the FSLG as a set of two single-mode ZLGs.

The study was conducted on a dynamic turntable with an angular velocity stabilisation accuracy of no worse than 0.0005%. The ZLG was rigidly fixed on the turntable faceplate so that its sensitivity axis was perpendicular to the Earth's surface. During the experiment with a small angular acceleration (0.01 deg s^{-2}), the angular velocity Ω of the turntable faceplate was changed in the range from –8.5 to +8.5 deg s^{-1} and the frequency output signal Ω_{out} of the gyroscope, corresponding to the angular velocity, was recorded. The measure-

ment results were presented as a dependence of Ω_{out} on the frequency Ω, where Ω is equal to the angular velocity divided by the output signal period value (Figs 1–4).

Figure 1 shows the output characteristic of a FZLG with a periodic frequency bias, recorded in the absence of a desynchronising signal. The dotted line in the figure shows the angular velocity corresponding to the frequency bias amplitude. At this scale, the output signal dependences for each of the modes practically merge with the output characteristic of the FZLG. On the FZLG output characteristic, as in the two-frequency ZLG, parametric synchronisation bands are clearly visible in the form of horizontal steps following through 1 kHz, as well as a large nonlinearity of the characteristic near the frequency bias amplitude. Following the tradition, parametric synchronisation bands will be further referred to as dynamic locking bands, in contrast to static locking bands in laser gyroscopes with a constant frequency bias.

Figure 2 shows, on an enlarged scale, part of the output characteristic of the FZLG with a periodic frequency bias without an additional desynchronising signal at angular rotation velocities close to the frequency bias amplitude, and the output characteristics of virtual single-mode ZLGs for each of the orthogonal modes. At this scale, one can observe the difference between the output characteristics obtained in the

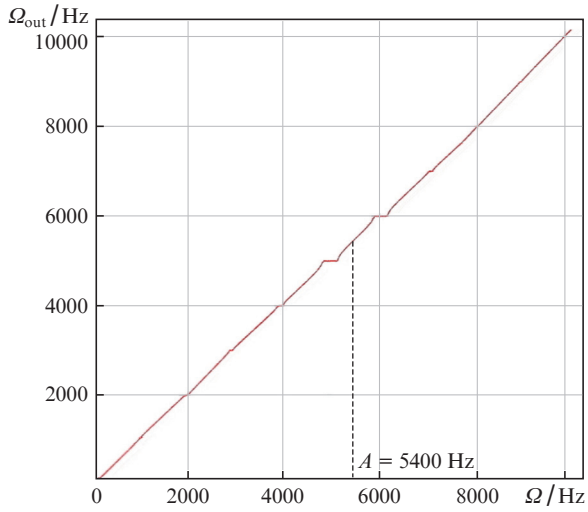

Figure 1. (Colour online) Output characteristic of the FZLG with a periodic square-wave frequency bias without an additional desynchronising signal.

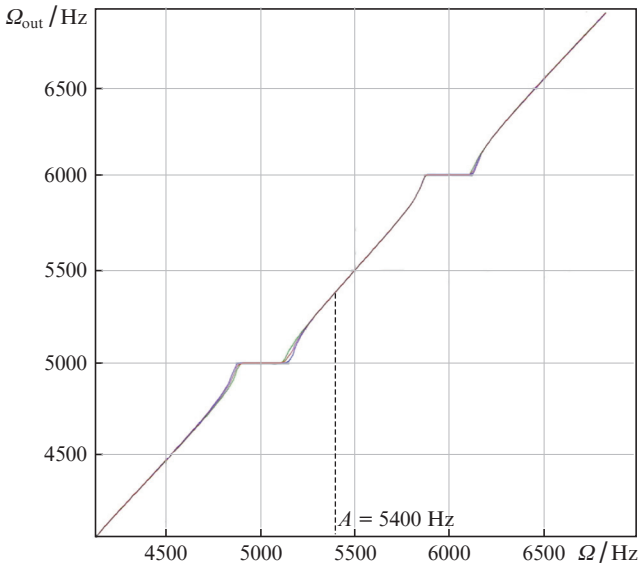

Figure 2. (Colour online) Output characteristic of the FZLG with periodic frequency bias without an additional desynchronising signal at angular rotation velocities close to the frequency bias amplitude (red curve), and output characteristics of virtual single-mode ZLGs (green curve refers to the "+" ZLG mode, and blue curve refers to the "–" ZLG mode).

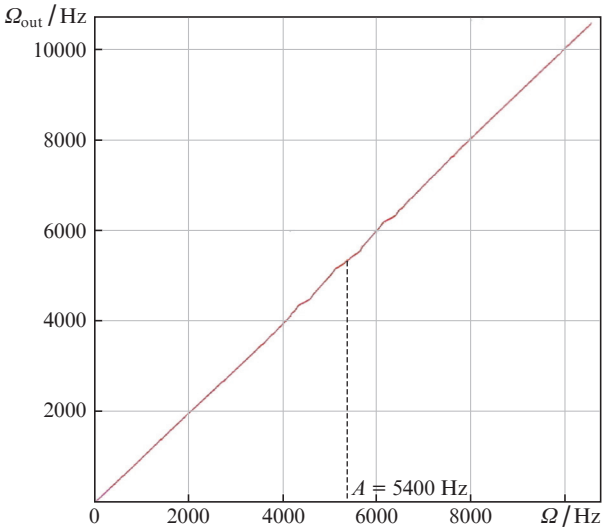

Figure 3. (Colour online) Output characteristic of the FZLG with a periodic frequency bias and an additional 'slow meander' desynchronising signal.

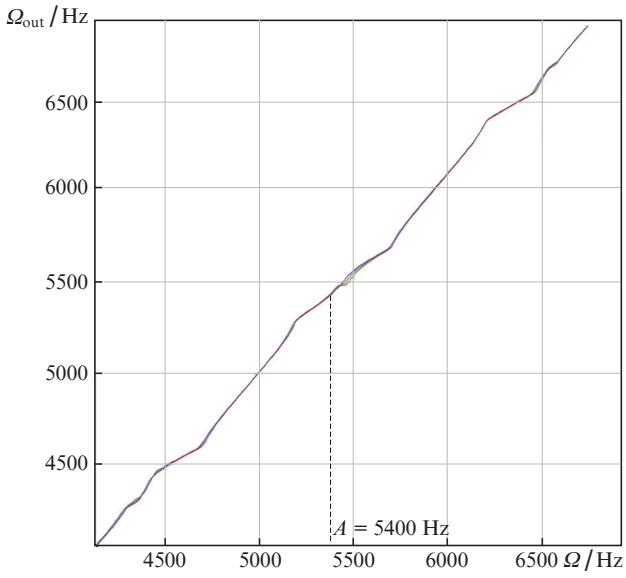

Figure 4. (Colour online) Output characteristic of the FZLG with a periodic frequency bias and an additional 'slow meander' desynchronising signal at angular rotation velocities close to the frequency bias amplitude (green curve refers to the "+" mode, blue curve, to the "–" mode, and red curve, to the FZLG as a whole).

single-mode regime and the output characteristic of a four-frequency ZLG.

The output characteristic of the FZLG with a periodic frequency bias and an additional desynchronising 'slow meander' signal in the same range of angular velocities is shown in Fig. 3. The same output characteristic at angular rotation velocities close to the frequency bias amplitude is shown on an enlarged scale in Fig. 4. As can be seen from Figs 3 and 4, due to low-frequency modulation, dynamic bands are reduced so much that they cease to be distinguished even on an enlarged scale, and in place of dynamic bands formed by FM, nonlinearities with inclined steps remain.

3. Analysis of the obtained results

There are no correctly obtained expressions in the literature for the output characteristic of FZLGs with an alternating-sign frequency bias, taking into account the coupling of counterpropagating waves through backscattering. In work [7], expressions are given for the frequency differences of counterpropagating waves in a ring laser with an alternating-sign frequency bias in the form of a meander in the four-frequency generation regime for the case when the coupling of counterpropagating waves can be neglected. The expressions have been obtained for the resonator tuning which is an operating one for the FZLG and characterised by the fact that the frequency differences of the counterpropagating waves in modes with orthogonal polarisations are equal in absolute value. For simplicity, it is assumed in work [7] that the modes with orthogonal polarisations have the same basic parameters: the scale factor and zero offsets. Generalising these expressions to the case of modes with different scale factors and zero offsets, we obtain

$$
\begin{aligned}
f_A^+ &= k_A(\Omega + \Delta\Omega_A) - K_{\mathrm{L}}(H+h)\frac{\Delta L}{\lambda} + K_H(H+h)(H+h),\\
f_B^+ &= k_B(\Omega + \Delta\Omega_B) - K_{\mathrm{L}}(H+h)\frac{\Delta L}{\lambda} - K_H(H+h)(H+h),\\
f_A^- &= k_A(\Omega + \Delta\Omega_A) + K_{\mathrm{L}}(H-h)\frac{\Delta L}{\lambda} - K_H(H-h)(H-h),\\
f_B^- &= k_B(\Omega + \Delta\Omega_B) + K_{\mathrm{L}}(H-h)\frac{\Delta L}{\lambda} + K_H(H-h)(H-h).
\end{aligned}
\tag{1}
$$

Here f_A^+ is the frequency difference (beat frequency) of counterpropagating waves in mode A at a positive sign of the alternating-sign magnetic field intensity H of the frequency bias (we conditionally call the corresponding half-cycle of the frequency bias positive); f_B^+ is the beat frequency of counterpropagating waves in mode B in the positive half-cycle of the frequency bias; f_A^- is the beat frequency of counterpropagating waves in mode A at the opposite direction of H (negative half-cycle of the frequency bias); f_B^- is the beat frequency of counterpropagating waves in mode B in the negative half-cycle of the frequency bias; h is the amplitude of the alternating-sign magnetic field that modulates the frequency bias amplitude; $K_{\mathrm{L}}(H+h)$ is the coefficient of the beat frequency dependence on the perimeter detuning value ΔL in the positive half-cycle of the frequency bias; $K_{\mathrm{L}}(H-h)$ is the coefficient of the beat frequency dependence on ΔL in the negative half-cycle of the frequency bias; $K_H(H+h)$ is the coefficient of the beat frequency dependence on the magnetic field intensity in the positive half-cycle of the frequency bias, $K_H(H-h)$ is the coefficient of the beat frequency dependence on H in the negative half-cycle of the bias; k_A and k_B are the FZLG scale factors for longitudinal modes A and B; Ω is the angular rotation velocity; and $\Delta\Omega_A$ and $\Delta\Omega_B$ are the zero offsets of the output FZLG characteristic for modes A and B. For brevity, equations (1) are written only for the positive half-cycle of the slow meander.

Taking advantage of the smallness of a slowly varying magnetic field compared to the amplitude of the alternating-sign field (in our case, it is 20 or more times smaller), we expand the coefficients K_{L} and K_H in Eqns (1) into a Taylor series with respect to h. Restricting ourselves to the first order of expansion, we obtain an expression for the combination of difference frequencies averaged over a period, which specifies the angular rotation velocity:

$$
\begin{aligned}
f_\Omega &= (f_A^+ + f_B^+ + f_A^- + f_B^-)/2 = k_A(\Omega + \Delta\Omega_A)\\
&\quad + k_B(\Omega + \Delta\Omega_B) + \frac{\Delta L}{\lambda}\frac{\mathrm{d}K_{\mathrm{L}}(H)}{\mathrm{d}H}h.
\end{aligned}
\tag{2}
$$

With the perimeter adjustment system (PAS) of the ring laser being in operation, the last term in formula (2) vanishes since the PAS maintains $\Delta L = 0$, and f_Ω can be represented as

$$
f_\Omega = \Omega(k_A + k_B) + k_A\Delta\Omega_A + k_B\Delta\Omega_B. \tag{3}
$$

Introducing the notations $k = (k_A + k_B)/2$, $\Delta k = k_A - k_B$, $\Delta\Omega_{AB} = (\Delta\Omega_A + \Delta\Omega_B)/2$, $\delta\Omega_{AB} = \Delta\Omega_A - \Delta\Omega_B$, we can write expression (3) as

$$
f_\Omega = 2k\Omega + 2k\,\Delta\Omega_{AB} + \delta\Omega_{AB}. \tag{4}
$$

Since $\Delta k \ll k$ in a laser gyroscope, the last term in (4) can also be neglected. As a result, we have

$$
f_\Omega = 2k\Omega + 2k\,\Delta\Omega_{AB}. \tag{5}
$$

Equation (5) implies that, given the approximations made, the FZLG scale factor is equal to the sum of the scale coefficients, and the zero offset in the FZLG is equal to the half-sum of zero offsets for individual modes. This makes it possible to use the results of the study on the coupling of counterpropagating waves through backscattering, obtained for two-frequency lasers when analysing the experimental results of studying the output characteristic of the FZLG.

In a ZLG with a periodic alternating frequency bias operating in the generation regime of a single longitudinal mode (two-frequency regime), the output characteristic (the beat frequency dependence on the angular rotation velocity) has nonlinearities due to the coupling of counterpropagating waves through backscattering [8–11] (schematically shown in Fig. 5). They manifest themselves as dynamic locking bands at frequencies being multiples of the frequency bias switching frequency (Fig. 5a), as well as in the form of a scale factor nonlinearity that reaches a maximum at angular velocities corresponding to the frequency bias amplitude (Fig. 5b). As can be seen from Figs 1 and 2, a similar pattern is observed in a FZLG.

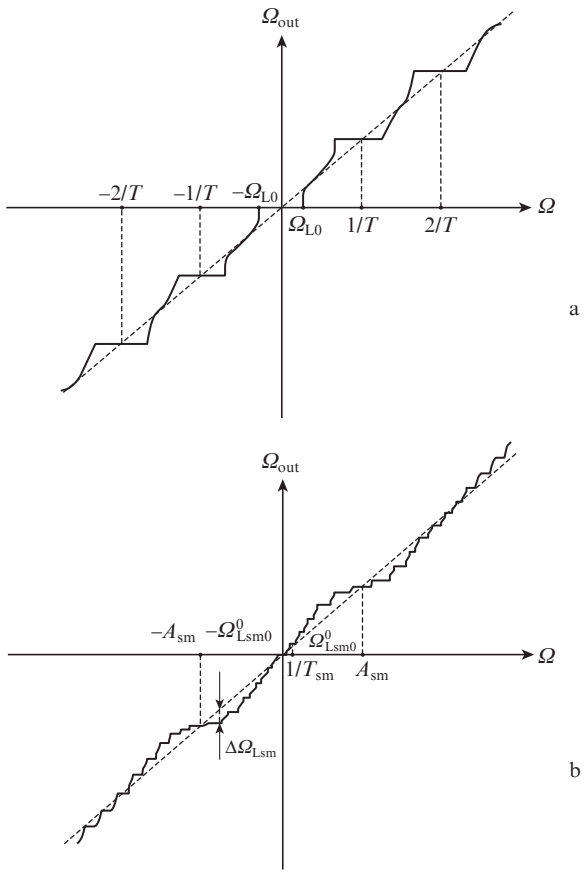

Figure 5. Output characteristics of the ZLG with a periodic frequency bias at low angular rotation velocities (a) without an additional desynchronising signal and (b) using an additional 'slow meander' desynchronising signal.

According to works [9, 10], the half-widths of the zero, even, and odd dynamic bands are written in the form

$$\Omega_{Li} = \Omega^0_L \left|\sin\left(\frac{\pi A T}{2}\right)\right|, \; i = 0, 2, 4, \ldots,$$
$$\Omega_{Li} = \Omega^0_L \left|\cos\left(\frac{\pi A T}{2}\right)\right|, \; i = 1, 3, 5, \ldots, \quad (6)$$

and the root-mean-square value of the half-width of the even and odd dynamic bands Ω^0_L with an alternating-sign frequency bias in the form of meander is determined by the expression

$$\Omega^0_L = \frac{2\Omega_{L+}}{\pi T A}\sqrt{1 + \pi^2 \tau A}, \quad (7)$$

where Ω_{L+} (Hz) is the half-width of the static locking band for a given mode, determined by dissipative backscattering centres; A (Hz) is the frequency bias amplitude for this mode; T (s) is the commutating period of the bias; and τ (s) is the duration of the bias switching front.

As the rotation frequency increases, the half-widths of the dynamic bands begin to grow rapidly as they approach the frequency bias amplitude [12].

In our case, the theoretical estimate of the half-widths of the dynamic bands gives the root-mean-square values of $\Omega^{0r}_L \approx 38$ Hz and $\Omega^{0l}_L \approx 41$ Hz, while the ratio of the widths of even and odd bands is $\Omega_{L0}/\Omega_{L1} \approx 1.33$. The experimentally obtained values are: $\Omega^{0r}_L \approx 27$ Hz, $\Omega^{0l}_L \approx 32$ Hz, and $\Omega_{L0}/\Omega_{L1} \approx 1.36$. The theoretical estimate of the half-width ratio of the locking bands of the same order for different modes $\Omega^{0r}_L/\Omega^{0l}_L$ is 0.93, while the experimental value of the ratio $\Omega^{0r}_L/\Omega^{0l}_L$ is 0.85. Thus, estimates of the dynamic characteristics using expressions for two-frequency FLGs give not only a qualitative, but also a good quantitative description of the ZLG characteristic nonlinearity caused by the coupling of counterpropagating waves through backscattering. The noticeably lower value of the absolute values of the half-widths of the dynamic locking bands observed in the experiment is apparently due to the desynchronising effect of the turntable rotation nonuniformity. The widths of the ZLG synchronisation bands coincide with the widths of modes with smaller locking. This indicates that mutual mode locking is not observed. At the same time, the nonlinearity of the characteristic is determined by the bands of the mode with greater locking.

Inside the dynamic bands, the ZLG output signal is $\Omega_{out} = i/T$, $i = 0, 1, 2, 3, \ldots$; outside of dynamic bands

$$\Omega_{out} \approx \frac{i}{T} + \sqrt{\left(\Omega - \frac{i}{T}\right)^2 - \Omega^2_{Li}}, \text{ if } \Omega > i/T,$$

and

$$\Omega_{out} \approx \frac{i}{T} - \sqrt{\left(\Omega - \frac{i}{T}\right)^2 - \Omega^2_{Li}} \text{ at } \Omega < i/T,$$

i is the number of the nearest dynamic band.

As can be seen from the above expressions, the output signal deviation from the measured angular velocity is determined primarily by the half-width of the static locking band, which depends on the size and type of scattering sources on the Zeeman ring laser mirrors, as well as on the mode polarisation. For this reason, it can differ significantly for modes with orthogonal polarisations, which is manifested in the difference in their output characteristics (see Fig. 2). The same figure shows that the FZLG output characteristic is an average of the characteristics of the orthogonal modes, as it follows from expression (5). The same can be noted for the relative nonlinearity of the scale factor $\Delta k/k$ [13]:

$$\frac{\Delta k}{k} = \frac{\Omega^2_{L+}}{2(\Omega^2 - A^2)} + \frac{\Omega^2_{L-}(\Omega^2_g + \Omega^2 - A^2)}{2[(\Omega + A)^2 + \Omega^2_g][(\Omega - A)^2 + \Omega^2_g]}. \quad (8)$$

Here Ω_{L+} (Hz) is the half-width of the static locking band for a given mode, determined by dissipative backscattering centres; A (Hz) is the bias frequency amplitude for this mode; Ω_{L-} (Hz) is the coefficient characterising the output characteristic distortion due to the coupling of counterpropagating waves, determined by conservative backscattering centres; and Ω_g (Hz) is the limit cycle strength of the ring laser. Note that, as shown in work [14], Ω_{L+} and Ω_{L-} depend on the distance between the mirrors, i. e., on the number of the longitudinal mode on which generation occurs. The dependences are periodic, with the amplitude of change in Ω_{L+} up to 30% from the average value, and the amplitude of the change in Ω_{L-} up to 80% from the average value.

Thus, the values of Ω_{L+} and Ω_{L-} for longitudinal modes with opposite circular polarisations can differ significantly. Accordingly, the nonlinearities of the output characteristics will also be different.

4. Linearization of the FZLG output characteristic using a slow meander

The results obtained in Section 3 indicate that all desynchronization methods used in two-frequency ZLGs can be effectively used for FLGs [11–13, 15]. Consider the linearization of the FZLG output characteristic using a slow meander – an alternating-sign magnetic field usually synchronised with the main field of the frequency bias (the so-called fast meander) but having a much lower amplitude and frequency.

After the SM introduction, small residual bands remain on the output characteristic (Fig. 5b), the root-mean-square half-widths of which are determined by the expression

$$\Omega^0_{\mathrm{L}smi} = \frac{2\Omega_{\mathrm{L}i}}{\pi T_{\mathrm{sm}} A_{\mathrm{sm}}}, \tag{9}$$

where A_{sm} and T_{sm} are the amplitude and period of the slow meander; and i is the number of the dynamic locking band. From (9) we find $\Omega^0_{\mathrm{Lsm0}} = 0.02$ Hz so that this band cannot be distinguished on experimental dependences.

In this case, the dynamic bands from FM turn into bands of the characteristic with a half slope, which is clearly seen in Fig. 3. The widths of these bands are determined by the width of the dynamic bands of the mode with greater static locking.

Provided that the angular velocity Ω is less than A_{sm}, the centres of the residual bands lie on the curve described by the function

$$\Omega_{\mathrm{out}} = \frac{1}{2}\left(\sqrt{(A_{\mathrm{sm}} + \Omega)^2 - \Omega^2_{\mathrm{L}i}} - \sqrt{(A_{\mathrm{sm}} - \Omega)^2 - \Omega^2_{\mathrm{L}i}}\right). \tag{10}$$

Hence, provided that $\Omega_{\mathrm{L}i} \ll A_{\mathrm{sm}}$ and $\Omega \ll A_{\mathrm{sm}}$, the shift of the characteristic is

$$\Delta\Omega_{\mathrm{Lsm}} = \Omega_{\mathrm{out}} - \Omega \approx \frac{1}{4}\frac{\Omega^2_{\mathrm{L}i}}{(A_{\mathrm{sm}} - \Omega)} \approx \frac{1}{4}\frac{\Omega^2_{\mathrm{L}i}}{A_{\mathrm{sm}}}. \tag{11}$$

The total error of the zero band position is

$$\Delta\Omega_{\mathrm{sm0}} = \frac{1}{4}\frac{\Omega^2_{\mathrm{L}0}}{A_{\mathrm{sm}}} + \frac{2\Omega_{\mathrm{L}0}}{\pi T_{\mathrm{sm}} A_{\mathrm{sm}}}. \tag{12}$$

The FZLG output characteristics using SM are shown in Figs 3 and 4. It can be seen that the SM introduction not only linearizes the FZLG output characteristic in terms of dynamic bands, but also reduces the scale factor deviation from the average value near the angular rotation velocity equal to the bias frequency amplitude.

5. Conclusions

The FZLG output characteristic is an average one over the output characteristics of each of the neighbouring longitudinal generation modes. For its linearization, conventional methods are effective, previously well-tested on the ZLG with the generation of a single longitudinal mode, in particular, the introduction of a slow meander. This makes it possible to significantly reduce the FZLG output characteristic nonlinearity associated with dynamic synchronisation bands at low angular rotation velocities, and to multiply reduce the scale factor nonlinearity at angular velocities close to the frequency bias amplitude.

References

1. Azarova V.V., Golyaev Yu.D., Dmitriev V.G. *Quantum Electron.*, **30**, 96 (2000) [*Kvantovaya Elektron.*, **30**, 96 (2000)].
2. Azarova V.V., Golyaev Yu.D., Saveliev I.I. *Quantum Electron.*, **45**, 171 (2015) [*Kvantovaya Elektron.*, **45**, 171 (2015)].
3. Milikov E.A. Cand. Diss. (M., MIPT, 2020).
4. Broslavets Yu.Yu., Fomichev A.A., Ambartsumyan D.M., Polukeev E.A. *Materialy 27-i mezhdunar. konf. po integrirovannym navigatsionnym sistemam* (Proc. 27th Int. Conf. on Integrated Navigation Systems) (St. Petersburg, 2020) p. 280.
5. Broslavets Yu.Yu., Fomichev A.A., Polukeev E.A., Ambartsumyan D.M., Egorov R.O. *Materialy 26-i mezhdunar. konf. po integrirovannym navigatsionnym sistemam* (Proc. 26th Int. Conf. on Integrated Navigation Systems) (St. Petersburg, 2019) p. 232.
6. Statz H., Dorschner T.A., Holtz M., Smith I.W., in *Laser Handbook* (Elsevier, 2013) Vol. 4, ch. 3, p. 229.
7. Varenik A.I., Gorshkov V.N., Grushin M.E., Ivanov M.A., Kolbas Yu.Yu., Saveliev I.I. *Quantum Electron.*, **51** (3), 276 (2021) [*Kvantovaya Elektron.*, **51** (3), 276 (2021)].
8. Klimontovich Yu.L. (Ed.) *Volnovye i fluktuatsionnye protsessy v lazerakh* (Wave and Fluctuation Processes in Lasers) (Moscow: Nauka, 1974).
9. Khoshev I.M. *Sov. J. Quantum Electron.*, **10**, 544 (1980) [*Kvantovaya Elektron.*, **7**, 953 (1980)].
10. Khromykh A.M. *Elektron. Tekh. Ser. 11: Laz. Tekh. Optoelektron.*, **53** (1), 26 (1990).
11. Golyaev Yu.D., Kolbas Yu.Yu., Tikhmenev N.V., Khokhlov N.I. *Elektron. Tekh. Ser. 11: Laz. Tekh. Optoelektron.*, **40** (4), 46 (1986).
12. Gorshkov V.N., Grushin M.E., Lariontsev E.G., Saveliev I.I., Khokhlov N.I. *Quantum Electron.*, **46**, 1061 (2016) [*Kvantovaya Elektron.*, **46**, 1061 (2016)].
13. Golyaev Yu.D., Telegin G.I., Tolstenko K.A., Yaremenko S.O. *Elektron. Tekh. Ser. 11: Laz. Tekh. Optoelektron.*, **56** (4), 17 (1990).
14. Azarova V.V., Golyaev Yu.D., Kuznetsov E.V. *Giroskopiya i Navigatsiya*, **28**, No. 14 (111), 71 (2020).
15. Golyaev Yu.D., Kolbas Yu.Yu., Tolstenko K.A., Naida O.N., Chubar A.V. *Elektron. Tekh. Ser. 11: Laz. Tekh. Optoelektron.*, **52** (4), 41 (1989).